Sensors & Diagnostics

ROYAL SOCIETY OF CHEMISTRY

COMMUNICATION

View Article Online
View Journal | View Issue

Cite this: *Sens. Diagn.*, 2022, **1**, 709

Received 17th February 2022,
Accepted 9th May 2022

DOI: 10.1039/d2sd00028h

rsc.li/sensors

Turn-on fluorescent sensors for Cu-rich amyloid β peptide aggregates†

Yiran Huang, Liang Sun and Liviu M. Mirica *

Protein misfolding and metal dishomeostasis are two key pathological factors of Alzheimer's disease. Previous studies have shown that Cu-mediated amyloid β (Aβ) peptide aggregation leads to the formation of neurotoxic Aβ oligomers. Herein, we report a series of picolinic acid-based Cu-activatable sensors, which can be used for the fluorescence imaging of Cu-rich Aβ aggregates.

The formation of extracellular amyloid plaques containing the amyloid β (Aβ) peptide is one of the pathological hallmarks of the brains of Alzheimer's disease (AD) patients.[1,2] Remarkably high concentrations (up to 20–50 μM) of Cu and Zn have been found within these amyloid plaques,[3,4] and several studies have explored the interactions of metals with monomeric Aβ peptides and their correlation with amyloid plaques and reactive oxygen species formation.[5–11] These studies show that Cu can slow down the aggregation of $A\beta_{42}$ and reduce fibrilization to a large extent, and it is considered that Cu(II) ions can stabilize the $A\beta_{42}$ oligomer species.[12–14] In this regard, novel molecules that can modulate the interaction of Cu ions with the soluble $A\beta_{42}$ species and alleviate their neurotoxicity may serve as novel therapeutic agents for AD.[15–20]

In addition to the development of new therapeutic agents, it is also highly important to detect the Cu-containing Aβ species in AD. A number of fluorescent sensors have been developed to probe biological copper fluxes.[21–25] These reporters can achieve high selectivity and signal-to-noise responses for Cu ion imaging, from cellular to tissue to whole animal settings.[21,26–28] However, only a few of these probes were utilized in detecting labile copper pools in AD,[29,30] even though countless studies have shown the copper homeostasis is dramatically disrupted. In this regard, to understand and probe the Cu-mediated Aβ aggregation process, it is significantly crucial to develop Cu–Aβ specific probes. Herein, we synthesized a series of Cu-based activatable sensors aimed to potentially detect the Cu–Aβ species *in vitro* and *ex vivo*. For the molecular design, we drew inspiration from Chan *et al.* who have reported the use of a 2-picolinic ester fragment that readily hydrolysed in the presence of Cu(II) but not with other divalent metal ions.[25] By linking the picolinic ester moiety with the Aβ-binding molecular fragments, Cu(II) ions can rapidly catalyze the hydrolysis of the ester bond to generate the highly fluorescent Aβ binding molecules *in vitro* (Fig. 1). Interestingly, the Cu-responsive sensors can also promptly react with Cu–Aβ oligomers and fibrils, resulting in a significant fluorescence turn-on, and indicating that the probes are able to detect Cu–Aβ species *in vitro*. To confirm the Aβ binding specificity of the probes, brain sections from transgenic 5xFAD mice were stained with the developed sensors. As expected, when the brain sections were only stained with the compounds, the fluorescence images show

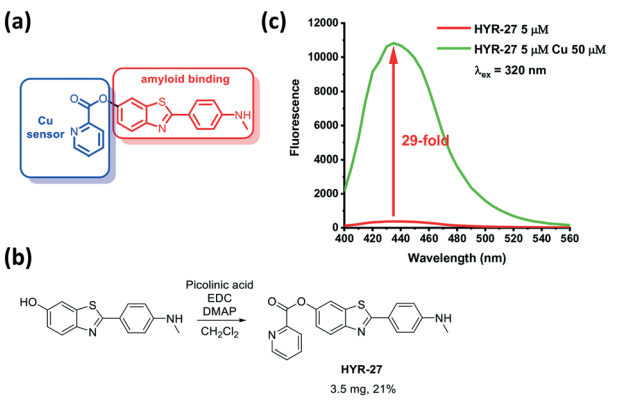

Fig. 1 a) Design and b) synthesis of Cu-based activatable sensor **HYR-27**; c) fluorescence turn-on effect of **HYR-27** in the presence of Cu(II); [**HYR-27**] = 5 μM, [Cu] = 50 μM, pH 7.4 PBS.

Department of Chemistry, University of Illinois at Urbana-Champaign, 600 S. Mathews Avenue, Urbana, IL 61801, USA. E-mail: mirica@illinois.edu

† Electronic supplementary information (ESI) available: Experimental procedures, spectroscopic data, and copies of NMR spectra. See DOI: **https://doi.org/10.1039/d2sd00028h**

that the sensor has a poor ability to detect amyloid plaques, given the low fluorescence intensity. However, upon the addition Cu(II) ions to the medium, followed by exhaustive washing of the free unbound Cu ions, the fluorescence images clearly indicate that the Cu-responsive sensors are activated by the Aβ-bound Cu(II) ions and release highly fluorescent amyloid binding fluorophores, which can specifically label the native amyloid plaques in the 5xFAD brain sections.

To detect Cu(II) in various Aβ species, the developed fluorescence probes such as **HYR-27** include two components: a Cu(II)-responsive 2-picolinic ester group that chelates Cu(II) ions and selectively activates the ester bond for hydrolysis (Fig. 1),[25,31] and a widely-used Aβ-binding molecular fragment derived from Pittsburgh compound B (PiB), which has high fluorescence intensity and can strongly interact with the Aβ fibrils.

To evaluate the copper-responsive activity of the probe, we firstly performed the Cu turn-on assay in PBS, using physiologically relevant Cu concentrations typically employed in *in vitro* Aβ-binding studies.[12–19] With the attachment of the picolinic ester moiety, the fluorescence intensity of the probe is dramatically quenched. However, when **HYR-27** was treated with Cu(II) ions, the fluorescence intensity significantly increased ~29 fold (Fig. 1 and S4†), indicating that the compound can coordinate to Cu(II) to facilitate the hydrolysis reaction and enhance the fluorescence intensity.

Then, we explored the Cu-activatable ability of **HYR-27** in the presence of various Aβ species. When the compound was treated with Aβ fibrils only, no fluorescence enhancement was observed after 30 min incubation. However, when Cu–Aβ fibrils were added to the solution, the fluorescence intensity dramatically increased, likely due to the rapid Cu(II)-catalysed hydrolysis reaction (Fig. 2). Addition of excess Cu(II) ions to the solution led to a further increase in the turn-on effect (~26 fold) to a fluorescence intensity similar to the one observed in the presence of only Cu(II) ions (Fig. 1). Furthermore, since Cu(II) ions were shown to stabilize the formation of Aβ oligomers, which are the most neurotoxic species *in vivo*, it is also crucial to also investigate if the developed probe can also detect Cu–Aβ oligomers. As a result, we first treated the compound with Aβ oligomers only. Similar to the Aβ fibril studies, no obvious turn-on effect was observed after 30 min incubation. Excitingly, when Cu(II) was added to the solution, the fluorescence intensity significantly increased, indicating that the probe can compete with the Aβ oligomers to chelate Cu(II) and facilitate the hydrolysis reaction to release the highly fluorescent PiB probe (Fig. 2). Importantly, the Cu-mediated hydrolysis of the picolinic ester fragment is slower in the presence of the Aβ aggregates (Fig. S4†), confirming that the Cu ions are indeed bound to the Aβ aggregates in these *in vitro* studies, and thus mimicking the *in vivo* conditions. Overall, the Cu-dependent fluorescence turn-on studies with or without various Aβ species clearly demonstrate that the developed probes can be efficiently activated by Cu(II), Cu(II)–Aβ fibrils, and Cu(II)–Aβ oligomers, exhibiting appreciable fluorescence turn-on *in vitro*.

To further explore the Aβ-binding affinity and Cu-activatable activity of **HYR-27**, we also performed fluorescence staining studies on brain sections from 11 month-old transgenic 5xFAD mice.[17] Firstly, the brain sections were only stained with **HYR-27**, and the low fluorescence intensity images show that the compound cannot efficiently detect amyloid plaques (Fig. 3), which is consistent with the *in vitro* studies. To mimic the Cu-rich environment, we first treated the brain sections with 50 μM Cu(II), followed by extensive washings with the buffer to remove any unbound Cu ions. Excitingly, performing the brain section staining following these treatment steps clearly shows that the fluorescence intensity significantly increased after the incubation with Cu(II), indicating that **HYR-27** was rapidly hydrolysed to form PiB, which can strongly bind to

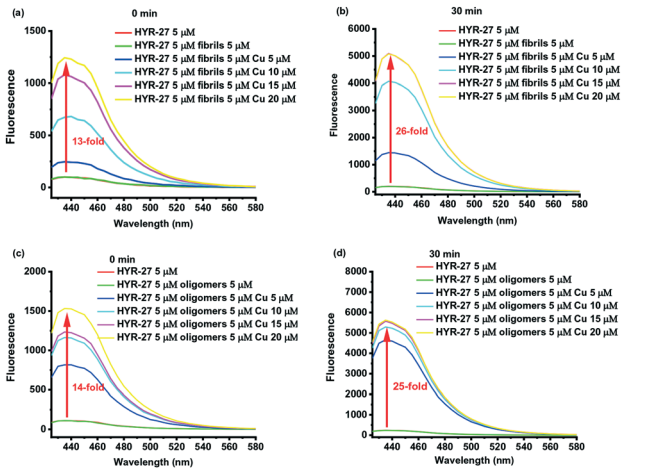

Fig. 2 Cu(II) fluorescence turn-on studies of **HYR-27** toward Aβ fibrils after a) 0 min and b) 30 min; Cu(II) fluorescence turn-on studies of **HYR-27** toward Aβ oligomers after c) 0 min and d) 30 min. [**HYR-27**] = 5 μM, [Aβ] = 5 μM, [Cu] = 0–20 μM in PBS (pH =7.4).

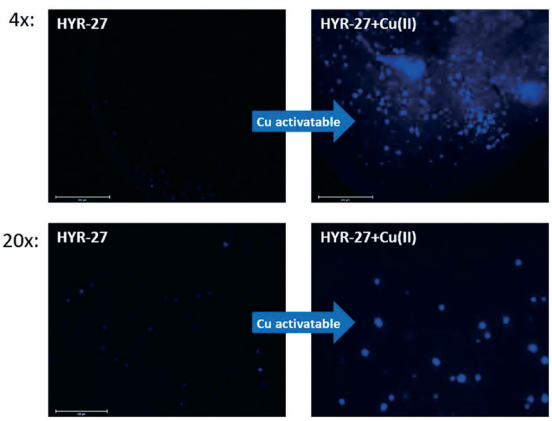

Fig. 3 Fluorescence microscopy images of 5xFAD mice brain sections incubated with compounds **HYR-27** (left panel) and **HYR-27** + Cu (right panel). [**HYR-27**] = 5 μM, [Cu] = 50 μM. Scale bar (20×): 125 μm.

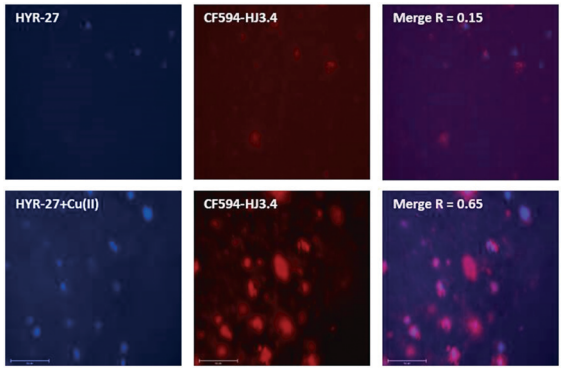

Fig. 4 Fluorescence microscopy images of 5xFAD mice brain sections incubated with compounds **HYR-27** (top left panel), **HYR-27** + Cu(II) (bottom left panel), and HJ3.4 (middle panels), and merged images (right panel). [**HYR-27**] = 5 μM, [Cu] = 50 μM, [HJ3.4] = 1 μg ml^{-1}. Scale bar: 125 μm.

the native amyloid plaques in the presence of Aβ-bound Cu(II) ions.

To further confirm the Aβ binding specificity, the brain sections were first stained with **HYR-27** or **HYR-27** + Cu(II), and sequentially immunostained with CF594-labeled HJ3.4 antibodies, which can bind to all Aβ species.[17] The fluorescence images show that while **HYR-27** does not show any colocalization with the HJ3.4 antibodies, in the presence of Cu(II), the hydrolysed product of **HYR-27** shows a significantly increased fluorescence intensity that is colocalized with the HJ3.4 antibodies (Fig. 4), showing that **HYR-27** has a high Cu-responsive ability that could be utilized to detect the Cu–Aβ amyloid plaques present in the 5xFAD brain sections.

Since the chelation of Cu(II) can facilitate the hydrolysis of the picolinic ester bond, a strong Cu(II)-binding chelator, Me_2HTACN, was introduced to the **HYR-27** fragment, to generate **HYR-27-TACN** (Fig. 5). However, when Cu(II) was added to **HYR-27-TACN**, the fluorescence intensity decreased

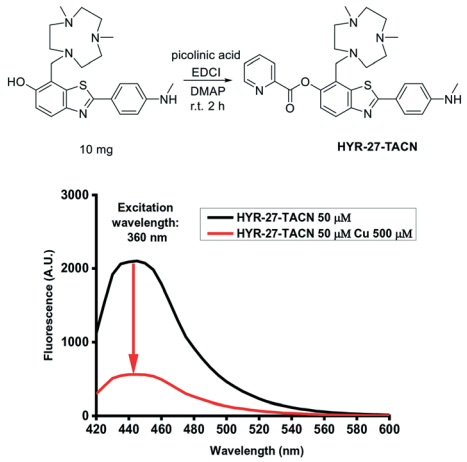

Fig. 5 Cu(II) fluorescence turn-on effects of **HYR-27-TACN**. [**HYR-27-TACN**] = 50 μM, [Cu] = 500 μM in PBS (pH = 7.4).

significantly, suggesting that in this case, Cu(II) ions bind strongly to the TACN group and cause paramagnetic quenching of the fluorescence intensity of **HYR-27-TACN**, instead of catalysing the hydrolysis reaction of the picolinic ester group. Thus, these results suggest that the use of strong Cu chelators may not be optimal for the design of Cu(II)-activatable fluorescent sensors, and a weaker Cu(II)-binding picolinic ester moiety may suffice to promote the hydrolysis of the ester bond.

After achieving promising results in which **HYR-27** can act as a Cu(II)-activatable fluorescent sensor, a series of curcumin derivatives with high Aβ-binding affinity and near-infrared (NIR) emission properties were functionalized with the Cu(II)-responsive picolinic ester fragment (Scheme 1 and Fig. S1–S3†). The syntheses of the curcumin precursors **YL-1**, **YL-3**, and **YL-5** were carried out by following previously reported procedures,[32] and the final Cu(II)-responsive curcumin derivatives **YL-2**, **YL-4**, and **YL-6** were synthesized *via* an EDC-mediated coupling reaction between 2-picolinic acid and the curcumin precursors.[31]

To confirm the Cu-activatable ability of the developed curcumin derivatives, fluorescence turn-on experiments were performed. Since the solubility of the compounds is poor in PBS, methanol was selected as the solvent to perform the Cu(II) turn-on assays. Notably, in the presence of Cu(II), the curcumin derivatives **YL-2**, **YL-4**, and **YL-6** exhibit a significant fluorescence turn-on signal, proving that the

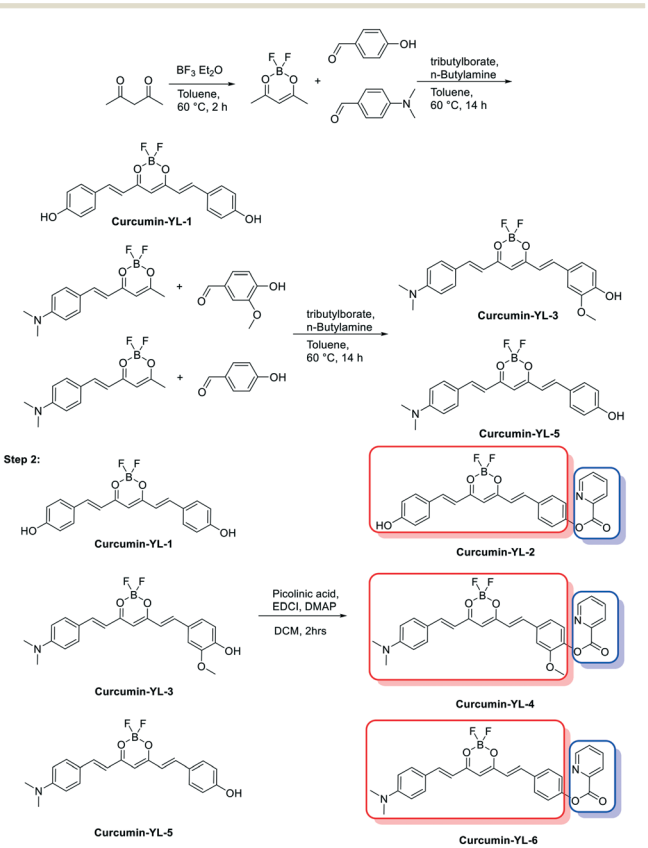

Scheme 1 Synthesis of curcumin cu(II)-activatable sensors.

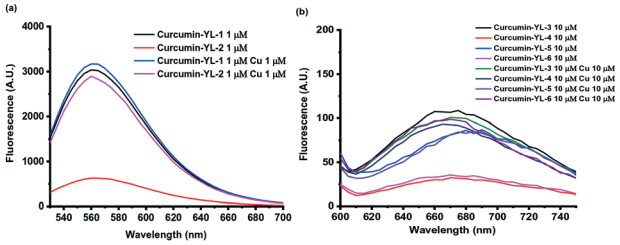

Fig. 6 Evaluation of Cu(II) fluorescence turn-on effects for a) **YL-1** and **YL-2**, and b) **YL-3**–**YL-6**. [**YL-X**] = 1 or 10 μM, [Cu] =1 or 10 μM in MeOH.

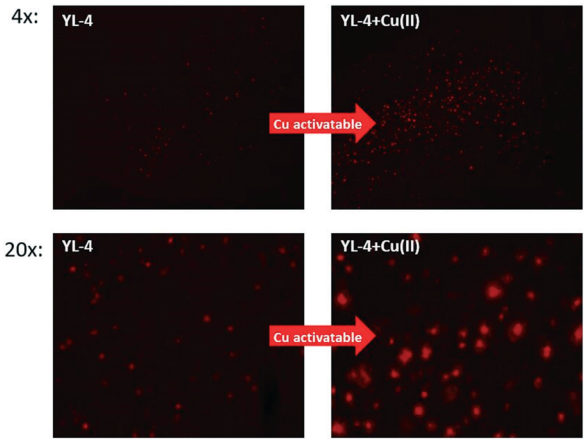

Fig. 7 Fluorescence microscopy images of 5xFAD mouse brain sections incubated with **YL-4** (left panels) and **YL-4** + Cu(II) (right panels). [**YL-4**] = 50 μM, [Cu] = 50 μM. Scale bar (20×): 125 μm.

developed curcumin-based compounds can be activated by Cu(II) ions (Fig. 6a and b, respectively).

To investigate the Cu-activatable activity of the curcumin derivatives towards amyloid plaques, fluorescence staining studies of 5xFAD brain sections were performed with **YL-4**, since **YL-4** exhibited the highest solubility in aqueous media. Upon staining of the brain sections with **YL-4** only, the fluorescence images show that **YL-4** can stain the amyloid plaques on the brain sections (Fig. 7). However, the fluorescence intensity of the **YL-4**-stained amyloid plaques is low, and it seems that **YL-4** can only stain the core regions of the amyloid plaques. By comparison, upon addition of Cu(II) to the staining solution of the 5xFAD brain sections, the fluorescence intensity of the compound-stained amyloid plaques significantly increases, indicating that **YL-4** is efficiently activated by Cu(II) to generate the more highly fluorescent curcumin derivative **YL-3**. Interestingly, upon incubation with **YL-4** and Cu(II), the resulting **YL-3** compound seems to also stain the periphery of the amyloid plaques where the Aβ oligomers and smaller Aβ aggregates are usually found, suggesting that these compounds have the potential to detect Cu–Aβ oligomers *ex vivo*. Overall, these brain section staining studies clearly demonstrate that **YL-4** can be utilized as a Cu-responsive sensor for the detection of Cu-rich Aβ aggregates of various sizes.

In conclusion, we rationally designed and synthesized a series of Cu-activatable sensors to detect Cu–Aβ species *in vitro* and *ex vivo*. With the introduction of the picolinate ester moiety attached to an Aβ-binding fragment, these developed fluorescent sensors can chelate Cu(II) to facilitate the hydrolysis of the ester bond and release the highly fluorescent Aβ-binding molecule *in vitro*. Furthermore, the Cu-responsive sensors can also react with Cu–Aβ oligomers and fibrils, resulting in a significant fluorescence turn-on, and indicating that the probes are able to detect Cu–Aβ species *in vitro*. To confirm the Aβ-binding specificity of the probes, transgenic AD mouse brain section imaging studies were also performed. As expected, if the brain sections were only stained with the compounds, the fluorescence images show that the sensor has a poor ability to detect amyloid plaques, exhibiting a low fluorescence intensity. However, in the presence of Cu(II) ions, the resulting fluorescence images clearly demonstrate that the sensors are activated by the Cu(II) ions and generate highly fluorescent amyloid-binding fluorophores, which can specifically label the amyloid plaques in the 5xFAD mouse brain sections. Overall, the developed Cu-activatable sensors can be utilized to detect Cu–Aβ species, both *in vitro* and *ex vivo*.

Conflicts of interest

There are no conflicts to declare.

References

1 2021 Alzheimer's disease facts and figures, *Alzheimer's Dementia*, 2021, 17, 327–406.
2 S. Tiwari, V. Atluri, A. Kaushik, A. Yndart and M. Nair, *Int. J. Nanomed.*, 2019, **14**, 5541–5554.
3 K. P. Kepp, *Coord. Chem. Rev.*, 2017, **351**, 127–159.
4 K. P. Kepp, *Chem. Rev.*, 2012, **112**, 5193–5239.
5 C. J. Maynard, A. I. Bush, C. L. Masters, R. Cappai and Q. X. Li, *Int. J. Exp. Pathol.*, 2005, **86**, 147–159.
6 M. A. Smith, G. Perry, P. L. Richey, L. M. Sayre, V. E. Anderson, M. F. Beal and N. Kowall, *Nature*, 1996, **382**, 120–121.
7 D. P. Smith, G. D. Ciccotosto, D. J. Tew, M. T. Fodero-Tavoletti, T. Johanssen, C. L. Masters, K. J. Barnham and R. Cappai, *Biochemistry*, 2007, **46**, 2881–2891.
8 B. Alies, C. Bijani, S. Sayen, E. Guillon, P. Faller and C. Hureau, *Inorg. Chem.*, 2012, **51**, 12988–13000.
9 J. T. Pedersen, J. Ostergaard, N. Rozlosnik, B. Gammelgaard and N. H. Heegaard, *J. Biol. Chem.*, 2011, **286**, 26952–26963.
10 S. Bagheri, R. Squitti, T. Haertle, M. Siotto and A. A. Saboury, *Front. Aging Neurosci.*, 2017, **9**, 446.
11 G. z. Eskici and P. H. Axelsen, *Biochemistry*, 2012, **51**, 6289–6311.
12 A. K. Sharma, S. T. Pavlova, J. Kim, D. Finkelstein, N. J. Hawco, N. P. Rath, J. Kim and L. M. Mirica, *J. Am. Chem. Soc.*, 2012, **134**, 6625–6636.

13 Y. Zhang, D. L. Rempel, J. Zhang, A. K. Sharma, L. M. Mirica and M. L. Gross, *Proc. Natl. Acad. Sci. U. S. A.*, 2013, **110**, 14604–14609.
14 A. K. Sharma, S. T. Pavlova, J. Kim, J. Kim and L. M. Mirica, *Metallomics*, 2013, **5**, 1529–1536.
15 A. K. Sharma, J. Kim, J. T. Prior, N. J. Hawco, N. P. Rath, J. Kim and L. M. Mirica, *Inorg. Chem.*, 2014, **53**, 11367–11376.
16 A. K. Sharma, J. W. Schultz, J. T. Prior, N. P. Rath and L. M. Mirica, *Inorg. Chem.*, 2017, **56**, 13801–13814.
17 H.-J. Cho, A. K. Sharma, Y. Zhang, M. L. Gross and L. M. Mirica, *ACS Chem. Neurosci.*, 2020, **11**, 1471–1481.
18 C. Esmieu, D. Guettas, A. Conte-Daban, L. Sabater, P. Faller and C. Hureau, *Inorg. Chem.*, 2019, **58**, 13509–13527.
19 C. Hureau, *J. Biol. Inorg. Chem.*, 2017, **22**, S230–S230.
20 H. J. Yu, W. Zhao, Y. Zhou, G. J. Cheng, M. Sun, L. Wang, L. Yu, S. H. Liang and C. Z. Ran, *Anal. Chim. Acta*, 2020, **1097**, 144–152.
21 T. Hirayama, G. C. Van de Bittner, L. W. Gray, S. Lutsenko and C. J. Chang, *Proc. Natl. Acad. Sci. U. S. A.*, 2012, **109**, 2228–2233.
22 S. Lee, C. Y. S. Chung, P. Liu, L. Craciun, Y. Nishikawa, K. J. Bruemmer, I. Hamachi, K. Saijo, E. W. Miller and C. J. Chang, *J. Am. Chem. Soc.*, 2020, **142**, 14993–15003.
23 K. J. Bruemmer, S. W. M. Crossley and C. J. Chang, *Angew. Chem., Int. Ed.*, 2020, **59**, 13734–13762.
24 D. A. Iovan, S. Jia and C. J. Chang, *Inorg. Chem.*, 2019, **58**, 13546–13560.
25 H. Li, P. Zhang, L. P. Smaga, R. A. Hoffman and J. Chan, *J. Am. Chem. Soc.*, 2015, **137**, 15628–15631.
26 M. Saleem, M. Rafiq, M. Hanif, M. A. Shaheen and S. Y. Seo, *J. Fluoresc.*, 2018, **28**, 97–165.
27 L. Zeng, E. W. Miller, A. Pralle, E. Y. Isacoff and C. J. Chang, *J. Am. Chem. Soc.*, 2006, **128**, 10–11.
28 D. W. Domaille, L. Zeng and C. J. Chang, *J. Am. Chem. Soc.*, 2010, **132**, 1194–1195.
29 B. Muthuraj, S. Layek, S. N. Balaji, V. Trivedi and P. K. Iyer, *ACS Chem. Neurosci.*, 2015, **6**, 1880–1891.
30 Y. Y. Yu, P. Wang, X. D. Zhu, Q. W. Peng, Y. Zhou, T. X. Yin, Y. X. Liang and X. X. Yin, *Analyst*, 2018, **143**, 323–331.
31 See ESI.†.
32 K. Liu, J. M. Chen, J. Chojnacki and S. J. Zhang, *Tetrahedron Lett.*, 2013, **54**, 2070–2073.